sustainability

MDPI

Article

Advancing Sustainability in Alloy Production: The Role of Recycled Materials and Barbotage in Enhancing EN AC-46000 Castings

Patryk Korban, Anna Wąsik and Beata Leszczyńska-Madej *

Faculty of Non-Ferrous Metals, AGH University of Krakow, 30 Mickiewicza Ave., 30-059 Krakow, Poland; anna.wasik@agh.edu.pl (A.W.)
* Correspondence: bleszcz@agh.edu.pl

Abstract: Aluminum recycling is a key pillar of sustainable metallurgy, protecting natural resources, reducing energy consumption by up to 15 times compared with primary aluminum production and significantly lowering the demand for raw materials. This article presents a comprehensive study on the impact of barbotage refining time and recycled scrap content on EN AC-46000 (AlSi9Cu3) alloy, covering the entire process from the initial ingot to the final casting, contributing to a circular economy. The input material consisted of varying proportions of pure ingots and scrap, with scrap content set at 80%, 70%, and 60%, respectively. Each material batch underwent different refining times: 0, 7, 9, and 15 min. Microstructural studies were conducted using light and scanning electron microscopy techniques. Additionally, pore distribution and their proportions within the material volume were analyzed using X-ray computed tomography. This study also examined hardness and gas content relative to the refining time. It was demonstrated that the refining process promoted microstructural homogenization and reduced porosity throughout the production process. Furthermore, extending the refining time positively impacted the reduction of porosity in thin-walled castings and lowered the gas emission level from the alloy, resulting in improved final product quality.

Keywords: sustainable metallurgy; aluminum recycling; barbotage refining; EN AC-46000 alloy; porosity; X-ray computed tomography; casting

check for updates

Academic Editors: Yasukazu Kobayashi and Rajesh Kumar Jyothi

Received: 8 March 2025
Revised: 17 May 2025
Accepted: 20 May 2025
Published: 22 May 2025

Citation: Korban, P.; Wąsik, A.; Leszczyńska-Madej, B. Advancing Sustainability in Alloy Production: The Role of Recycled Materials and Barbotage in Enhancing EN AC-46000 Castings. *Sustainability* **2025**, *17*, 4755. https://doi.org/10.3390/su17114755

Copyright: © 2025 by the authors. Licensee MDPI, Basel, Switzerland. This article is an open access article distributed under the terms and conditions of the Creative Commons Attribution (CC BY) license (https://creativecommons.org/licenses/by/4.0/).

1. Introduction

Aluminum–silicon-based alloys are widely used in the casting industry due to their excellent mechanical properties, corrosion resistance, and ease of casting. These alloys are essential for producing automotive parts, electronics housings, and various structural components that require a balance of strength, durability, and lightweight characteristics [1].

The growing emphasis on sustainability has driven increased utilization of recycled aluminum, offering both environmental and economic benefits. Recycling aluminum not only conserves natural resources but also reduces carbon emissions and energy consumption compared with virgin metal production. The primary raw materials for melting furnaces typically include virgin ingots, scrap metal, runners, risers, and foundry returns [2]. Virgin ingots provide a pure source of the alloy, while recycled materials, such as scrap, runners, and risers from previous casting processes, are reintroduced into the melting process. Aluminum can be recycled indefinitely without significant loss of its inherent properties, making production more cost-effective and environmentally friendly [3]. However, the

accumulation of impurities in recycled aluminum alloy streams poses a long-term compositional challenge to achieving high-quality castings, necessitating careful control during the melting process [4]. During melting, molten aluminum readily absorbs hydrogen from various sources, including the atmosphere, moisture in scrap materials, wet scraps, or moisture in refractory linings. This can negatively affect the material's mechanical properties [5]. Impurities can weaken the structure, reduce ductility, and lead to casting defects such as porosity. The primary concern in castings is the presence of hydrogen and oxygen, both of which are soluble in liquid aluminum [6]. The solubility of hydrogen in solid aluminum alloys is extremely low, causing dissolved hydrogen to be released as gas bubbles during solidification, resulting in macro porosity and microporosity in castings [7]. Conversely, oxygen contributes to the degradation of cast products under dynamic loads by promoting the formation of aluminum oxide (γ-Al_2O_3) [8]. These oxide films promote the nucleation and growth of fatigue cracks, ultimately weakening the casting [9]. Therefore, degassing the molten aluminum alloys before the casting process is essential for producing sound, high-integrity, and defect-free castings [10]. Despite these challenges, using recycled materials offers significant benefits. It reduces the demand for raw aluminum, which requires energy-intensive extraction processes, and it lowers production costs by decreasing the need for primary metal [11]. Additionally, recycling minimizes the environmental footprint of casting operations by reducing greenhouse gas emissions and energy consumption [12]. However, additional challenges in casting arise with the production of large and complex die castings, which introduce issues such as uneven material properties, increased defects, and residual stress accumulation. These factors can compromise mechanical performance and require advanced manufacturing solutions. A data-driven predictive model is necessary to optimize the design of super-sized thin-walled aluminum castings, ensuring improved structural integrity and minimization of defects [13].

The methodology for removing impurities from aluminum primarily involves two approaches: mechanical mixing devices and gas injection systems. Together, these methods effectively reduce impurity levels in the aluminum melt, improving the quality and integrity of the final castings [14]. To ensure high-quality castings from recycled materials, processes like barbotage (also known as gas bubbling) are essential. Barbotage is a melt refining technique where inert gases, such as argon or nitrogen, are bubbled through the molten aluminum [15]. This process serves several critical functions in producing defect-free castings, particularly when recycled materials are used. The primary role of barbotage is to remove hydrogen gas, which can dissolve in molten aluminum during the melting process and lead to porosity and other casting defects. The introduced gas bubbles are fragmented into very small bubbles by the high-speed rotation of the rotor. These fine bubbles float to the surface of the melt. As they ascend, which happens slowly due to their small size, hydrogen diffuses into the bubbles where the partial pressure of the hydrogen is effectively zero. This diffusion process allows the hydrogen dissolved in the melt to escape into the inert gas bubbles, which then rise to the surface and are released, thereby reducing the hydrogen content in the melt and minimizing the risk of porosity in the final castings [16,17]. This process directly supports sustainability by enabling higher recycled content without compromising material integrity. Optimizing barbotage parameters, including refining time, gas flow rate, and rotor speed, is essential for minimizing energy consumption and maximizing the efficiency of impurity removal [18]. Studies by Bhaskar et al. [19] and Gyarmati et al. [20] indicate that the most critical parameters for this process include gas flow rate (argon or nitrogen), rotor geometry, and bath temperature. A gas flow rate that is too low results in inadequate contact with the molten metal, reducing the efficiency of hydrogen and impurity removal. On the other hand, an excessively high flow rate can cause metal splashing and excessive heat loss. Research shows that higher

rotor speeds improve hydrogen removal but also increase heat loss, thereby prolonging the process. Elevated temperatures accelerate gas dissolution, shortening the refining time, but they also increase the risk of metal oxidation. When a higher proportion of scrap is used, optimizing both temperature and rotor speed becomes crucial for reducing the refining time. Gyarmati et al. [20] also noted that scrap content affects the alloy's chemical composition, which may necessitate adjustments to the required refining parameters, such as temperature and gas flow intensity. Shabestari et al. [21] observed that increasing the rotor speed and reducing the gas pressure improved gas removal, thus shortening the refining time. Additionally, the authors reported that a higher scrap content increased the levels of impurities and hydrogen in the melt, necessitating either a longer refining time or more intensive parameters, such as a higher gas flow rate. Choomgdo et al. [22] investigated the impact of the gas bubbling filtration treatment on microporosity variation and tensile properties of aluminum alloy. Their findings revealed that fractographic porosity in the specimens could be minimized under specific gas bubbling filtration conditions, primarily influenced by buoyant velocity, gas bubble absorption capacity, and the presence of oxide films. Additionally, volumetric porosity was significantly reduced with increased degassing time. Under optimal conditions, ultimate tensile strength and elongation improved compared with untreated samples. However, while extending the degassing time or excessive stirring led to the inclusion of bifilm oxides and an increase in fractographic porosity, the tensile properties of over-treated specimens remained comparable to those without treatment, attributed to the grain refinement achieved during the process. Gyarmati et al. [23] examined the impact of barbotage treatments combined with fluxing on the melt quality of an Al-Si-Mg-Cu casting alloy. The results indicated that barbotage, in conjunction with flux addition, is an effective method for removing inclusions and dissolved hydrogen, leading to a significant improvement in melt quality.

The combination of recycled materials and barbotage creates a synergistic effect in the production of aluminum alloy castings. While recycled aluminum reduces costs and environmental impact, barbotage ensures that casting quality is maintained by mitigating the risks associated with impurities. This approach contributes significantly to sustainability by promoting circular use of materials and reducing the carbon footprint associated with primary aluminum production. Despite numerous studies on aluminum scrap recycling, there is a lack of detailed data regarding the maximum amount of recycled scrap that can be added to the charge while maintaining the optimal mechanical and chemical properties of castings. This article focuses on the optimization of the refining process of EN AC-46000 alloy (AlSi9Cu3) using the bubbling technique. Although degassing is a well-established method for reducing gas porosity, processing techniques, particularly in the context of using recycled scrap, still require further improvement and remain the subject of intensive study. Unlike previous research, which primarily addressed low to moderate levels of scrap, this study demonstrates that up to 80% recycled aluminum scrap can be successfully utilized without substantial loss of mechanical performance. This challenges conventional limitations regarding scrap content and highlights the effects of high levels of recycled materials on microstructural properties. The main objective of this work was to optimize process parameters, such as refining time and scrap content, to achieve improved mechanical and microstructural properties while minimizing defects and maintaining acceptable costs. By showing that higher scrap content can be efficiently refined through optimized degassing, this study contributes to the development of more sustainable aluminum production with reduced reliance on primary raw materials.

2. Materials and Methods

In this study, the investigated material was EN AC-46000 (AlSi9Cu3) foundry aluminum alloy, produced from a combination of pure ingots and recycled scrap in varying proportions. The tested variants contained 80%, 70%, and 60% recycled scrap, respectively. The alloy's chemical composition, corresponding to the recycled scrap content, was analyzed using a Thermo Fisher (ARL)-3461 emission spectrometer (Thermo Fisher Scientific, Waltham, MA, USA). The obtained results are summarized in Table 1.

Table 1. Chemical composition of the examined EN AC-46000 (AlSi9Cu3) foundry aluminum alloy as a function of recycled scrap content (wt.%).

Element	Al	Si	Fe	Cu	Mn	Mg	Zn	Cr	Others
80% scrap metal	82.61	10.10	1.44	2.59	0.17	0.59	1.00	0.05	1.38
70% scrap metal	85.65	9.23	1.31	2.30	0.22	0.29	0.64	0.05	0.29
60% scrap metal	85.49	9.50	0.98	2.49	0.16	0.33	0.72	0.03	0.29
0% scrap metal	86.29	8.79	1.07	1.95	0.24	0.37	0.84	0.04	0.41

The composition of the alloy conformed to the PN-EN 1706 + A1:2022-01 standard [23]. Although slight variations in elements such as Cu and Mg were observed, their levels did not significantly exceed typical manufacturing tolerances. Considering the overall low content of Mg and the identical processing conditions applied to all samples, the influence of composition differences on the mechanical properties was considered minor compared with the effects of refining time and scrap content investigated in this study.

Each batch of material was subjected to different refining durations of 0, 7, 9, and 15 min. The scrap content levels (60%, 70%, and 80%) and refining times (0, 7, 9, and 15 min) were selected based on industrial practice and to explore process optimization within feasible operational limits. In commercial rotary degassing systems, such as the FDU Mini Degasser (Foseco International Limited, Tamworth, Staffordshire, UK) used in this study, refining durations typically range from 5 to 15 min depending on melt characteristics and process constraints. The 7 min time reflects a standard cycle applied in routine production at the partner foundry, while 15 min represents an upper operational limit beyond which heat loss and rotor degradation may outweigh benefits. An intermediate time of 9 min was chosen to assess the potential for optimizing melt quality while reducing gas consumption, energy usage, and equipment wear—factors that are essential from a cost-efficiency perspective. A schematic diagram of the barbotage process is presented in Figure 1. The melting process was carried out using an Inductotherm Europe Power-Trak CR induction furnace (Inductotherm Group Europe, Worcestershire, UK) with a maximum capacity of 1500 kg, operating at approximately 720 °C. To improve the quality of the molten metal, an FDU Mini Degasser was utilized for degassing, cleaning, and grain refinement. This process involved submerging a shaft-rotor assembly into the melt, initiating its rotation, and introducing argon gas through a channel in the rotor pin. The degassing procedure was conducted at a rotor speed of 500 rpm, with an argon flow rate of 20 L per minute. During each melting and refining cycle, the argon gas flow rate was monitored using the built-in flowmeter of the FDU Mini Degasser, which provided real-time readings. In case of any deviation, adjustments were made using the pressure regulator and flow control valve on the argon gas cylinder. This ensured stable and uniform degassing conditions throughout all the experiments. After melting, dross and oxides accumulating on the surface were systematically removed. This operation was repeated multiple times to obtain samples with different refining durations and recycled scrap contents.

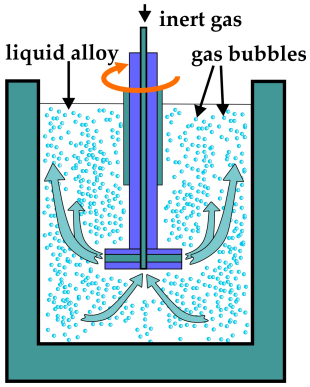

Figure 1. Schematic diagram of barbotage process.

Once the refining process was complete, samples were extracted from the molten alloy using a steel shank ladle at temperatures between 710 °C and 730 °C. The metal was then poured into a steel crucible and left to cool in air. The crucible dimensions were approximately 4 cm in height with a base diameter of 2.6 cm and a top diameter of 2.8 cm, resulting in an approximate sample volume of 39 cm^3. To determine the gas content, MK 3000 precision scales were employed.

In the subsequent stage of the study, castings were produced using a cold-chamber die-casting process. The Italpresse 550 SC die-casting machine (Italpresse S.P.A, Bagnatica, Italy) operated with a clamping force of 550 tons, and the piston injection speed was set at 3.2 m per second. The oil temperature, maintained by the temperature control unit, was regulated at 170 °C.

The microstructural analysis of the samples was conducted using optical microscopy (OLYMPUS GX51, Tokyo, Japan) and scanning electron microscopy (SEM) with a Schottky-type electron gun (SU-70, Hitachi Ltd., Tokyo, Japan), equipped with a NORAN System 7 (Thermo Scientific, Waltham, MA, USA) X-ray microanalysis system (EDS). Additionally, the hardness of the samples was evaluated using the Brinell method. A sintered carbide ball with a 2.5 mm diameter was applied with a load of 31.25 kgf, following the ASTM E10-18 standard [24]. The measurement duration was approximately 60 s, with six measurements performed for each sample. A static uniaxial compression test was then performed at room temperature using a Zwick Roell Z020 testing machine. For this purpose, sets of four cylindrical samples, each with a height-to-diameter ratio of 1.5, were prepared for each variant according to ASTM E-9 [25]. The compression test was carried out at a constant tool feed rate of 0.7 mm/s and was stopped upon reaching a permanent deformation of 45%.

The distribution and size of pores inside the samples and pressure castings were analyzed using an YXLON Y.MU2000-D X-ray and CT inspection system (YXLON International GmbH, Hamburg, Germany). The examinations were performed with a current intensity of 15 mA and an emission tube voltage of 120 kV. The measurement time was approximately 5 min per object, with a single voxel dimension of 0.4 mm, an active detector size of 200 mm × 200 mm, and a tube-to-detector distance of 795 mm, optimized for the measurements. The resolution of the X-ray matrix was 1000 × 1000 pixels. During testing, the object was placed in the chamber of the YXLON Y.MU2000-D tomograph on a platform that enabled movement relative to the X-ray emission tube and radiation detector as well as rotation around its axis. The radiation emitted by the tube was partially absorbed by the sample, analyzed by the detector, and converted into a digital image. As the sample was rotated on the platform, each rotation step was accompanied by the acquisition of a projection, facilitating the reconstruction of 3D models.

3. Results and Discussion

Below, in Figures 2–4, representative results of the microstructural analysis of the EN AC-46000 (AlSi9Cu3) alloy in the as-cast state are presented. The ingots were cast at a relatively low cooling rate. The resulting microstructure was coarse-grained, with a low amount of gas or mixed (gas-shrinkage) porosity. The microstructure consisted of an α-Al solid solution with silicon eutectic (α_{Al} + β_{Si}) and copper-rich phases characterized by a distinct golden color. The results of the SEM/EDS chemical composition analysis, presented as elemental distribution maps and point analyses (Figures 3 and 4), suggest that the copper-rich precipitates were probably θ (Al_2Cu) and W($Al_5Si_6Mg_8Cu_2$) phases. The W($Al_5Si_6Mg_8Cu_2$) phase was observed in eutectic form. Additionally, iron-rich phases, most probably α (AlFeSi) with the chemical formula Al_8Fe_2Si, are present in the microstructure. These phases exhibited acicular or plate-like morphologies.

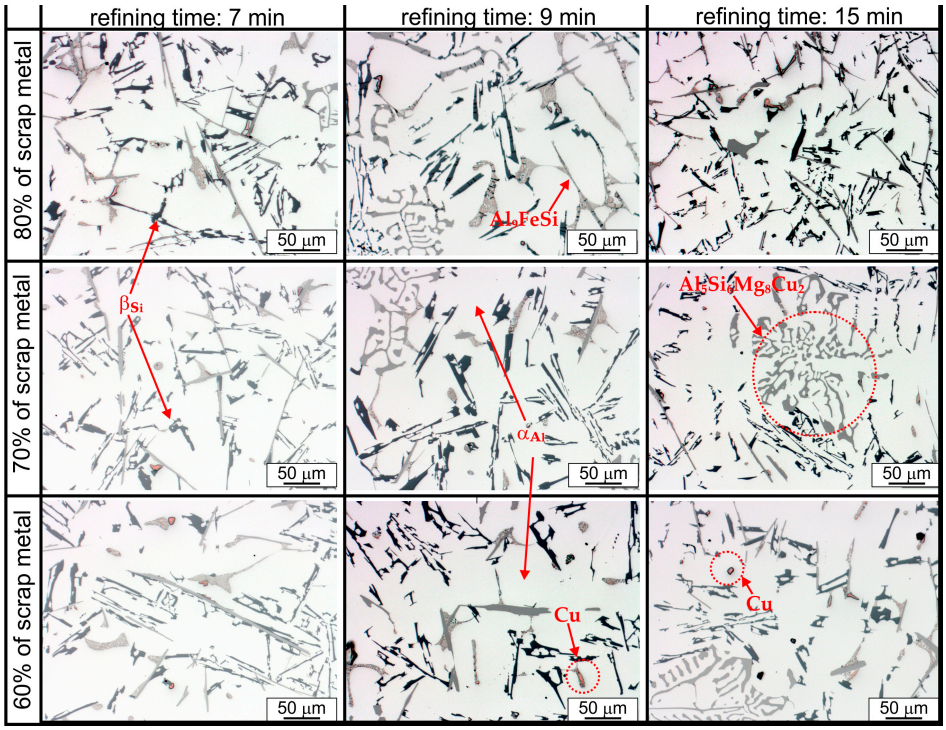

Figure 2. Microstructure of EN AC-46000 (AlSi9Cu3) ingot alloy as a function of recycled scrap content and refining time; LM.

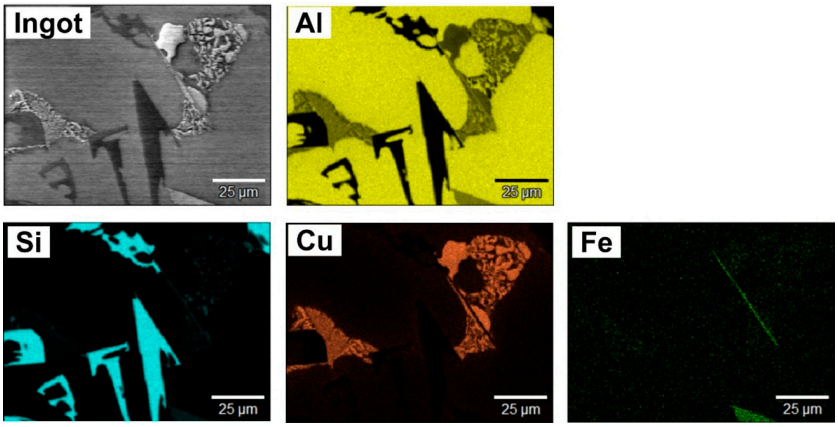

Figure 3. Microstructure of the EN AC-46000 (AlSi9Cu3) ingot alloy and chemical analysis in microarea; refining time—7 min, 70% scrap metal; SEM/EDS.

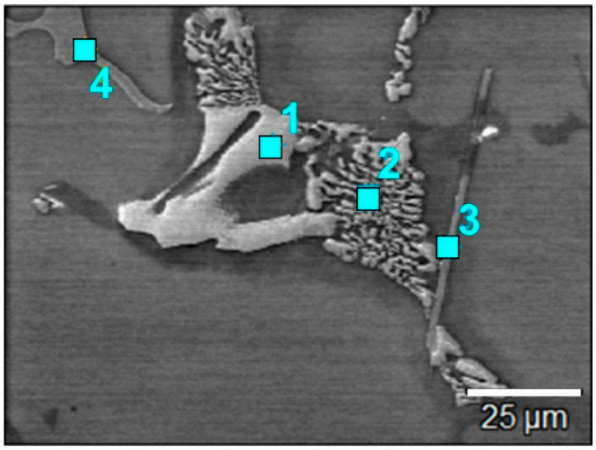

% mas.	Mg	Al	Si	Mn	Fe	Ni	Cu
1	0.00	33.84	0.00	0.00	0.00	10.19	55.97
2	3.01	57.70	3.66	0.00	0.00	0.00	35.64
3	0.00	50.50	14.81	2.65	30.29	0.00	1.75
4	0.00	53.61	9.46	8.81	23.46	0.00	4.65

Figure 4. Microstructure of the EN AC-46000 (AlSi9Cu3) ingot alloy and chemical analysis in microarea; refining time—15 min, 70% scrap metal; SEM/EDS.

One of the key quality parameters of aluminum castings is their gas content, which directly affects their mechanical properties, as does the presence of defects such as porosity. To assess the effectiveness of the refining process, a density index analysis was conducted, and the obtained results are presented in the graph in Figure 5 and in Table 2. Due to the specific characteristics of the process, density index measurements were conducted only on the ingots. Three measurements were performed for each variant. No significant discrepancies were observed between the individual variants. During the measurements, the melt temperature was carefully controlled within a specific range to prevent excessive dissolution of gas in the liquid metal, which could have led to oxidation and distorted the results [26]. The melting process temperature ranged from 719 to 746 °C. The obtained results clearly demonstrate a significant decrease in gas content with increasing duration of barbotage, regardless of the recycled scrap content in the alloy. The highest density index values were observed in metal samples that had not undergone refining. In these cases, the density index ranged from 14.4% to 17.04%, indicating substantial gas saturation in the alloy when the refining process was omitted. After refining, a significant reduction in gas content was observed. For samples containing 80% recycled scrap, the initial density index value was 17.04%, which decreased to 1.16% after 15 min of refining. A similar trend was noted for the alloy with 70% recycled scrap content, where the density index decreased from 14.4% to 1.37% after 15 min of refining. In the alloy with 60% recycled scrap, the density index values dropped from 15.63% to 1.43% after the same refining duration.

These findings clearly confirm that barbotage is an effective method for removing gases from the metal. Extending the refining time significantly reduced the gas content, regardless of the scrap content percentage, which is consistent with literature data on aluminum alloy refining methods. The authors of a previous study [27] demonstrated that 15 min of refining resulted in a density index reduction of approximately 90%. Furthermore, it was shown that a higher recycled scrap content is associated with a higher initial gas level, confirming that recycled scrap may be the primary source of gases in the alloy. Additionally, previous studies have emphasized that the effectiveness of barbotage is influenced by several factors, including the size of the gas bubbles, the degassing rotor speed, and the nature of the carrier gas used during the process [28,29]. For instance, helium and argon have been found to be more effective than nitrogen due to their lower

solubility in aluminum [30]. Other studies have also indicated that increasing the rotor speed enhances the removal of dissolved hydrogen but may lead to excessive turbulence, potentially causing re-oxidation and secondary contamination [31]. Another important factor influencing porosity in aluminum alloys is the presence of oxide films and inclusions, which act as nucleation sites for gas bubbles. Research has shown that oxide bifilms can significantly reduce fatigue life and impact mechanical properties even in well-refined alloys [32]. Furthermore, the impact of alloying elements on the efficiency of barbotage has been a subject of extensive research. Magnesium, for example, has been found to enhance hydrogen solubility in liquid aluminum, leading to increased gas porosity if not properly managed [33]. Conversely, strontium additions, commonly used for eutectic silicon modification, have been reported to alter bubble nucleation and affect the degassing kinetics [34].

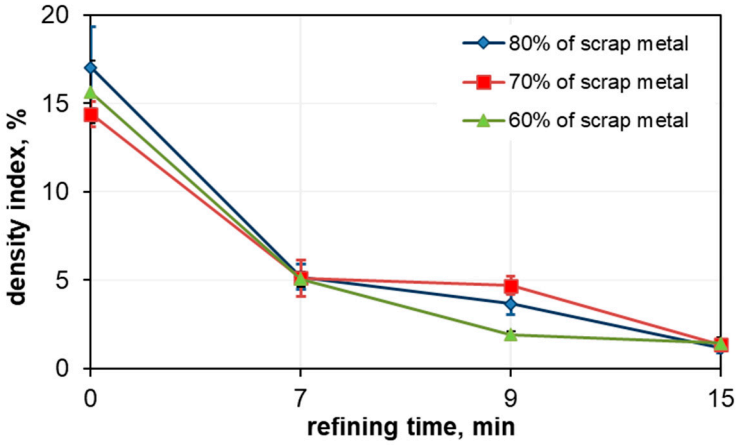

Figure 5. Effect of refining time and recycled scrap content on the density index.

Table 2. Density index and maximum pore value depending on recycled scrap content and refining time.

EN AC-46000 ($AlSi_9Cu_3$) Ingot Alloy						
	Recycled Scrap Content					
	80%		70%		60%	
Refining Time, Min	Density Index, %	Maximum Pore Value, mm^3	Density Index, %	Maximum Pore Value, mm^3	Density Index, %	Maximum Pore Value, mm^3
7	5.19	32.23	5.13	1165.01	5.06	7.35
9	3.66	292.97	4.7	1062.59	1.93	636.04
15	1.16	137.12	1.37	87.05	1.43	167.18

In the current study, 3D models of the samples were generated based on the conducted tomographic analysis. The obtained data for the ingots is summarized in Table 2 and, for selected variants, in X-ray CT images (Figure 6). Additionally, Table 2 provides a summary of the density index test results.

The ingots subjected to different durations of barbotage and containing varying amounts of recycled scrap exhibited significant differences in porosity volume depending on the process parameters; however, no single trend could be identified. For example, in ingots containing 60% recycled scrap refined for 7 min, the volume of the largest porosity was 7.35 mm^3 (Table 2). In contrast, in ingots refined for 9 min, the volume of the largest porosity increased significantly to 636.04 mm^3. This suggests that a longer refining time, despite reducing gas content, may lead to an increase in porosity volume. Extending the

refining time to 15 min resulted in a reduction of the largest porosity volume to 167.18 mm^3. A similar trend was observed in the alloy containing 80% recycled scrap.

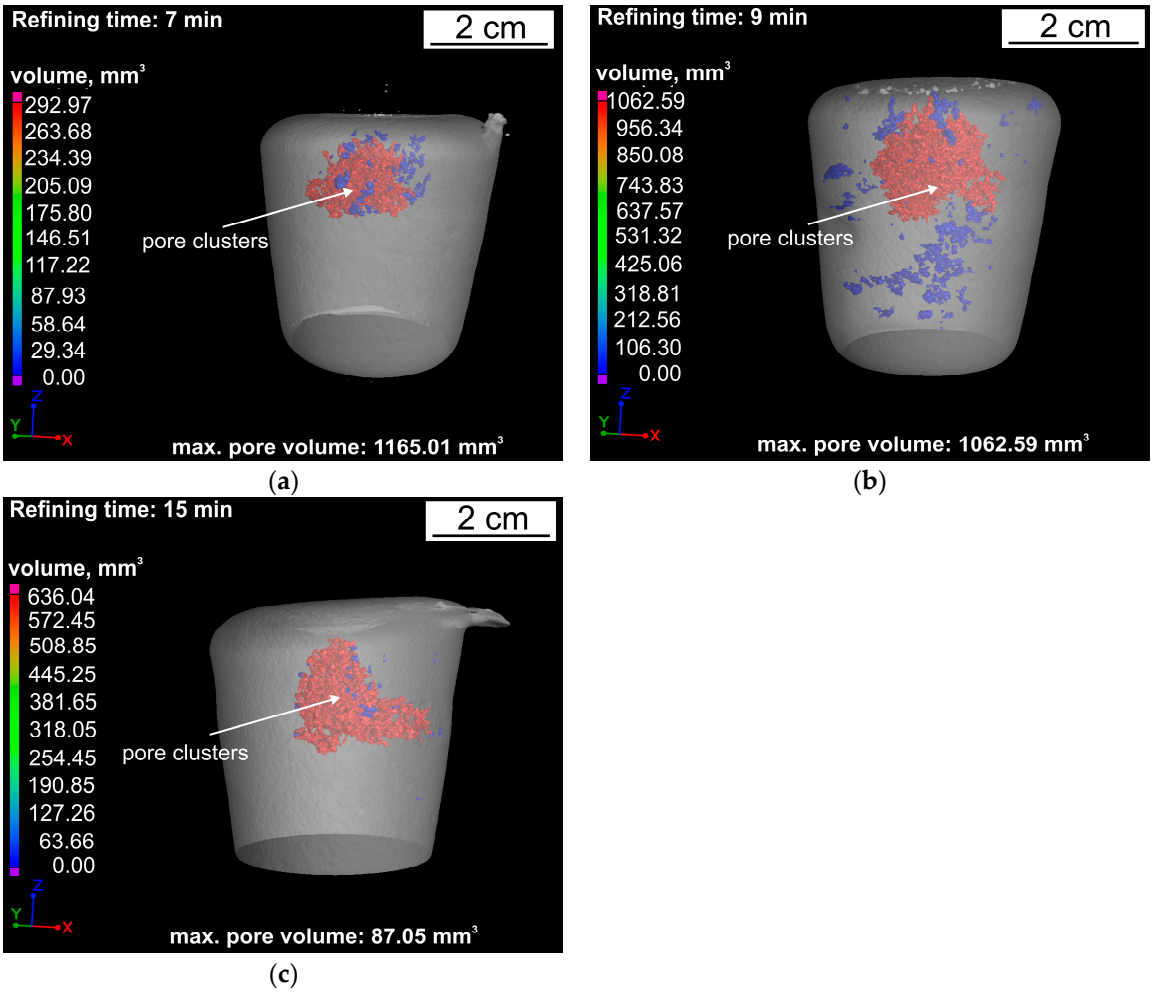

Figure 6. Casting model of the ingot considering recycled scrap content and refining time. The figure provides information on porosity: (**a**) refining time—7 min, recycled scrap content—70%; (**b**) refining time—9 min, recycled scrap content—70%; (**c**) refining time—15 min, recycled scrap content—70%; CT.

In the case of ingots with 70% recycled scrap, an increase in refining time led to a decrease in the volume of the largest porosity. After 7 min of refining, the largest porosity volume was 1165.01 mm^3, whereas after 15 min, it decreased to 87.05 mm^3 (Table 2, Figure 6). In all cases, prolonging the refining time resulted in a reduction in the density index of the ingots (Table 2). This reduction in density index with prolonged refining times aligns with findings from industrial assessments. For example, research evaluating refining efficiency during industrial degassing highlighted the importance of optimizing processing parameters to balance the effectiveness of degassing and minimize adverse effects such as rotor degradation and temperature drop [29].

The microstructure of the die-cast alloys exhibited distinct characteristics (Figures 7–9). The high cooling rate, reaching up to 100 °C/s, was reflected in the refinement of the microstructure, particularly the α_{Al} solid solution, the silicon eutectic (α_{Al} + β_{Si}), and the precipitation of iron-rich β (Al_9FeSi) phases with an undesirable needle-like morphology. This phenomenon is an effect of so-called undercooling modification. In the microstructure of die-cast alloys, polygonal precipitates were visible, which are most likely to have been Al(Fe,Mn,Cr)Si-type phases with non-stoichiometric compositions, as confirmed by the

chemical composition analysis (Figures 8 and 9). These precipitates form the so-called "sludge", which does not dissolve during remelting. During the alloy's solidification, these precipitates typically appeared in a solid state already at the pre-dendritic crystallization stage of the α_{Al} solid solution. Copper-rich precipitates exhibited a different morphology compared with those in the ingots—they did not form branched eutectics and were located at grain boundaries.

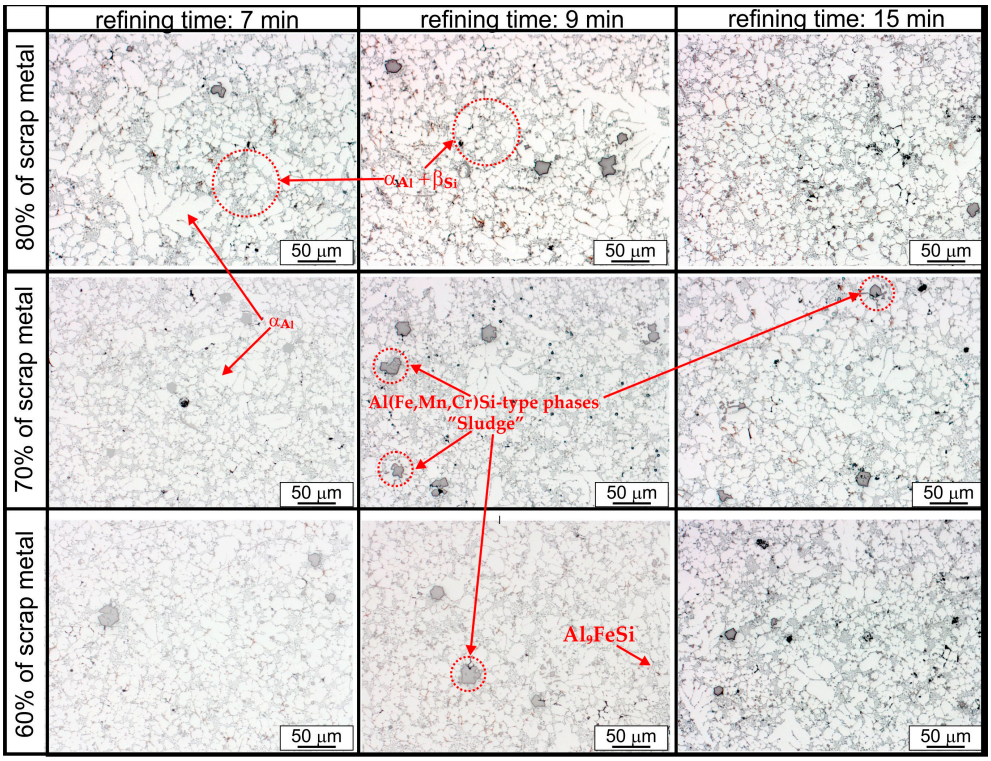

Figure 7. Microstructure of the EN AC-46000 (AlSi9Cu3) die-cast alloy depending on content of recycled scrap and refining time; LM.

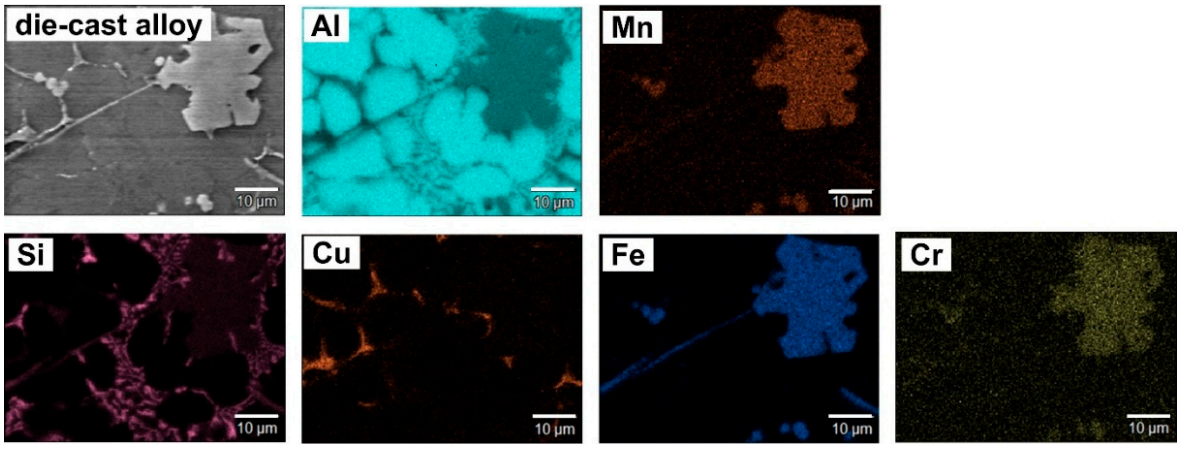

Figure 8. Microstructure of the EN AC-46000 (AlSi9Cu3) die-cast alloy and element distribution maps: Al, Mn, Si, Cu, Fe, Cr; refining time—7 min, 60% scrap metal; SEM/EDS.

Porosity in the die castings was significantly lower compared with the ingots (Figures 10–12). In all analyzed cases, the volume of the largest porosity was the smallest in the castings refined for 7 min and remained similar for all alloy compositions, ranging from 4.10 to 6.36 mm^3. With the exception of the casting containing 80% recycled scrap, extending the refining time to 9 min contributed to a reduction in the volume

of the largest porosity, with the lowest porosity observed in the casting containing 60% recycled scrap. Further extending the refining time to 15 min resulted in a reduction in the volume of the largest porosity only in the casting with 80% recycled scrap.

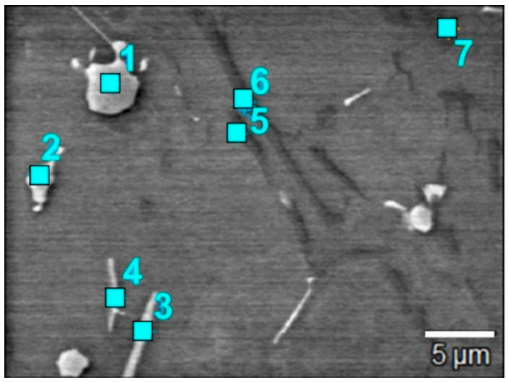

% mas.	Al	Si	Cr	Mn	Fe
1	54.87	9.09	4.90	2.09	29.05
2	53.55	9.07	5.69	1.59	30.09
3	48.66	20.99	0.00	0.00	30.34
4	91.15	4.31	0.00	0.00	4.54
5	96.05	3.95	0.00	0.00	0.00
6	15.96	84.04	0.00	0.00	0.00
7	29.52	70.48	0.00	0.00	0.00

Figure 9. Microstructure of the EN AC-46000 (AlSi9Cu3) die-cast alloy and chemical analysis in microarea; refining time—7 min, 60% scrap metal; SEM/EDS.

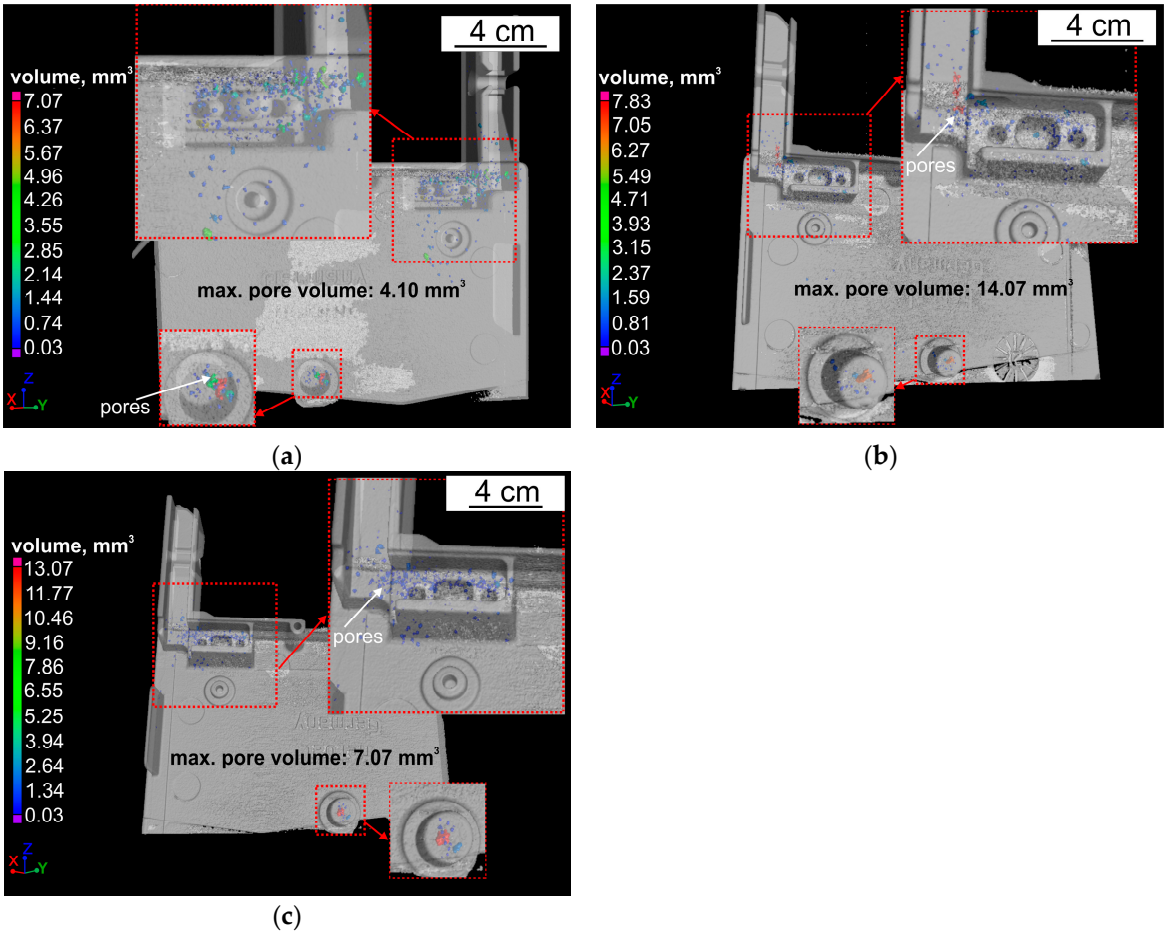

Figure 10. Casting model of the cassette cover for a roller shutter system, considering the recycled scrap content and refining time. The figure presents information on porosity: (**a**) refining time—7 min, recycled scrap content—80%; (**b**) refining time—9 min, recycled scrap content—80%; (**c**) refining time—15 min, recycled scrap content—80%; CT.

The results presented by Gyarmati et al. demonstrate that despite the reduction of gas porosity through the degassing process, shrinkage porosity remained present in ingot regions with an irregular structure, where shrinkage forces were greater, particularly in

areas where solidification was the slowest [20]. In die castings, the solidification process is significantly faster and more controlled, which limits the formation of shrinkage porosity. This type of porosity is more pronounced in ingots due to their slower solidification and larger dimensions.

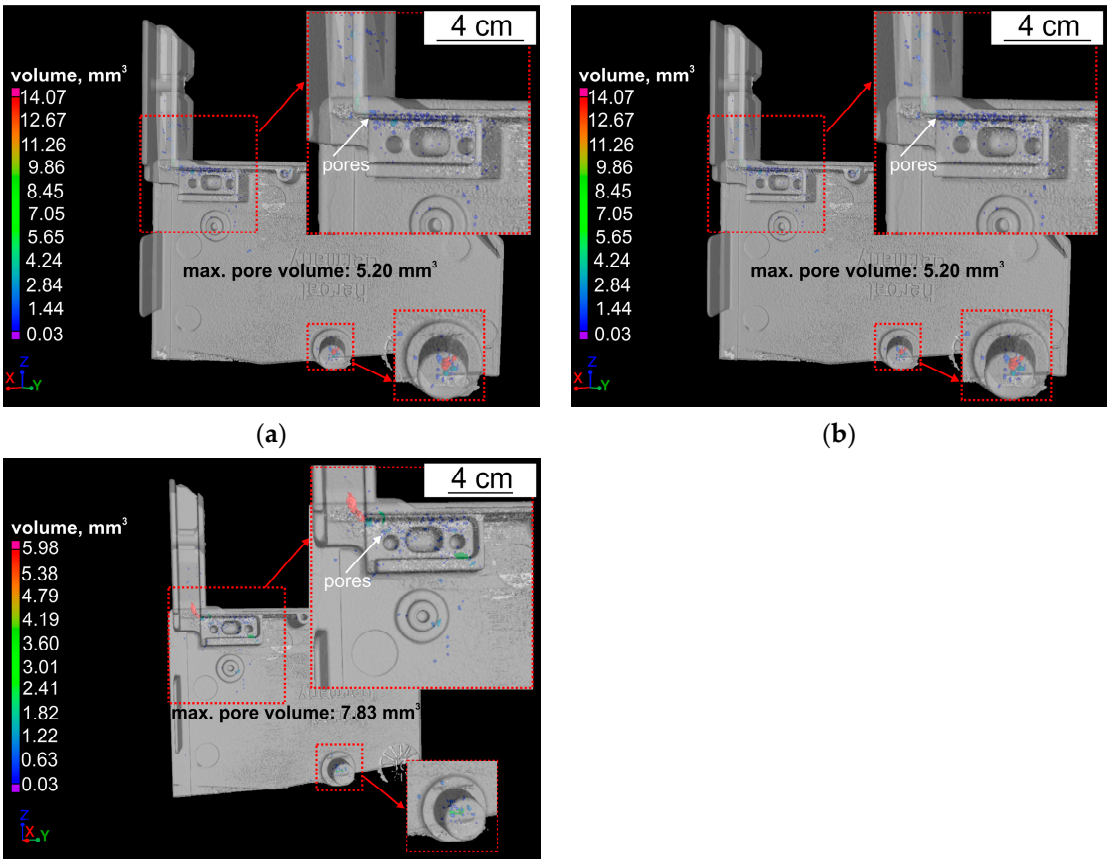

Figure 11. Casting model of the cassette cover for a roller shutter system, considering the recycled scrap content and refining time. The figure presents information on porosity: (**a**) refining time—7 min, recycled scrap content—70%; (**b**) refining time—9 min, recycled scrap content—70%; (**c**) refining time—15 min, recycled scrap content—70%; CT.

As evidenced by the obtained microstructural analysis results (Figure 7) and computed tomography scans (Figures 10–12), the die castings exhibited a more homogeneous microstructure and a lower degree of porosity, as a result of better control over the cooling and crystallization process. The ingots, on the other hand, showed higher porosity and gas entrapment, which was attributed to their shape and slower solidification process.

It is worth noting that inconsistent trends in porosity size with respect to refining time may not solely reflect the efficiency of the refining process itself, particularly in the case of castings obtained after transferring the melt to holding or workstation furnaces. Rather, they may be partially attributed to the deterioration of melt quality due to re-oxidation and bifilm formation during handling. When molten aluminum is poured or transferred under suboptimal atmospheric protection, oxide films can form on the surface and become entrained into the melt, creating bifilms. These bifilms can act as nucleation sites for porosity, even in conditions of low hydrogen content. The likelihood of such defects increases with extended treatment durations or multiple handling steps. Therefore, the observed variability in porosity under certain conditions should be interpreted with consideration of the refining parameters and also melt handling practices.

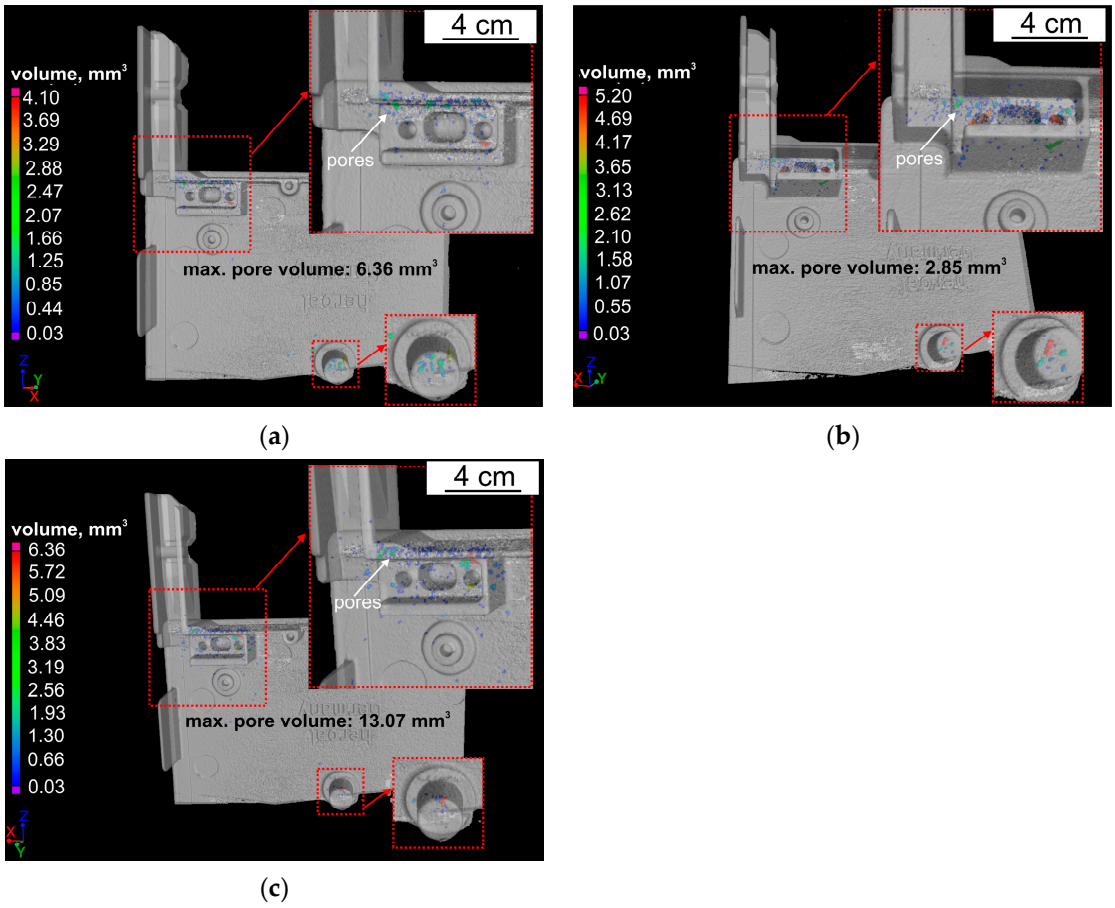

Figure 12. Casting model of the cassette cover for a roller shutter system, considering the recycled scrap content and refining time. The figure presents information on porosity: (**a**) refining time—7 min, recycled scrap content—60%; (**b**) refining time—9 min, recycled scrap content—60%; (**c**) refining time—15 min, recycled scrap content—60%; CT.

In order to determine the mechanical properties, Brinell hardness measurements and a uniaxial compression test were performed. The obtained results are presented in Figures 13 and 14. The hardness measurements of the ingots showed minor variations depending on the recycled scrap content and refining time, with values ranging from 77 to 81 HB. (Figure 13a). The hardness of the castings was significantly higher than that of the ingots, ranging from 98 to 101 HB, with any differences falling within the measurement error margin. These results indicate that the Brinell hardness was not sensitive to the refining process. The higher hardness of the die castings was primarily influenced by their microstructure, which is more homogeneous in castings than in ingots.

According to the literature, an increase in recycled scrap content in aluminum alloys often leads to a higher concentration of impurities such as iron, manganese, and copper. These impurities promote the formation of iron-rich phases, particularly the needle-like β-Al_5FeSi phase, which exhibits undesirable morphologies. Such morphological changes can contribute to increased shrinkage porosity and a subsequent decline in mechanical properties, including ultimate tensile strength (UTS), yield strength (YS), and elongation. For instance, in $AlSi_{10}MnMg$ alloys, raising the scrap content from 50% to 75% resulted in a notable decrease of 16% in both UTS and YS, along with an 18% reduction in elongation [35].

The graphs provided for both the ingots (Figure 13a) and the die-cast alloys (Figure 13b) illustrate the influence of refining time and scrap metal content on compressive strength at strain levels $\varepsilon = 0.05$ and $\varepsilon = 0.1$.

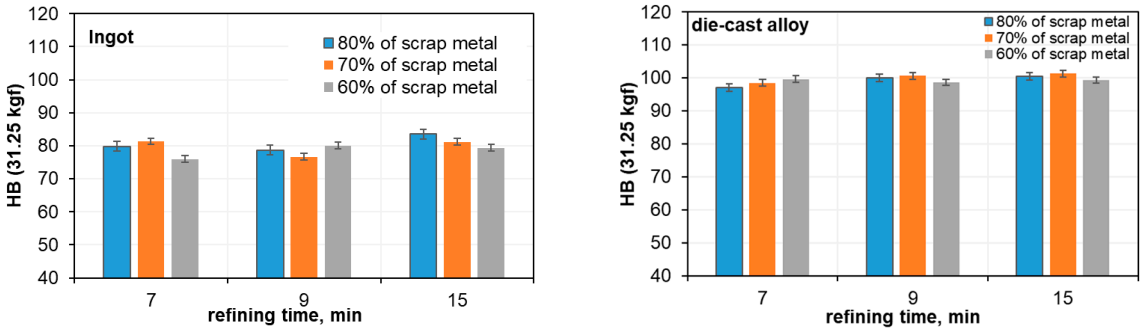

(**a**) (**b**)

Figure 13. Hardness measurement results as a function of refining time and recycled scrap content: (**a**) ingot, (**b**) die-cast alloy.

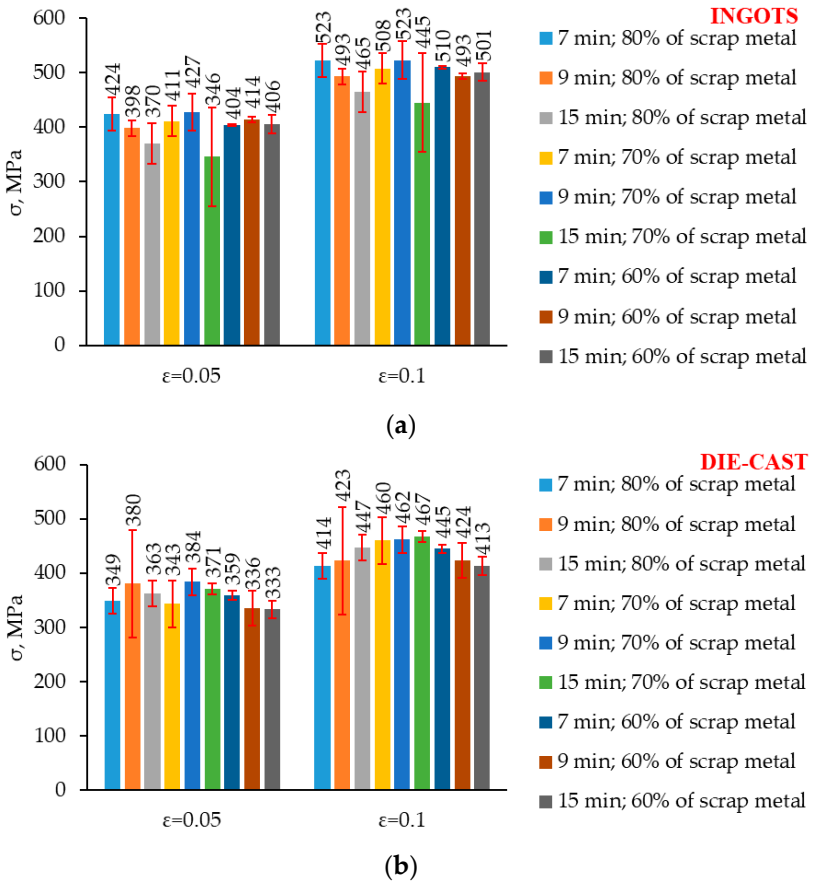

(**a**)

(**b**)

Figure 14. The average stress values for (**a**) ingots and (**b**) castings measured at 0.05 and 0.1 real strain.

The analysis indicates that increasing the scrap metal content generally leads to a decrease in mechanical strength, though this effect is modulated by refining time. For instance, in the ingot samples refined for 7 min, strength slightly increased with higher scrap content, from σ = 510 MPa at 60% scrap to 523 MPa at 80% scrap (ε = 0.1). Conversely, the die-cast variants under the same conditions exhibited a notable decrease, from σ = 445 MPa at 60% scrap to 414 MPa at 80% scrap. Scrap content significantly influences mechanical performance. While increasing recycled scrap content typically introduces more impurities, such as iron, the appropriate refining duration appears to mitigate this effect by promoting cleaner melts, reducing porosity, and ensuring better distribution of intermetallics [35]. At 80% scrap, alloys generally exhibit lower strength than those with 60% or 70% scrap content, suggesting that higher scrap proportions may compromise

mechanical integrity. For instance, at 15 min and 80% scrap, the ingot's strength was 370 MPa (ε = 0.05) and 465 MPa (ε = 0.1), whereas at 15 min and 60% scrap, these values were higher at 406 MPa and 510 MPa, respectively. The opposite trend was observed in the die-cast alloys with extended refining times (9, 15 min), where strength increased with higher scrap content, rising to 363 MPa and 447 MPa (15 min, 80% scrap) from 333 MPa and 413 MPa (15 min, 60% scrap), though a slight decrease was seen at ε = 0.05, possibly due to casting variability.

Overall, the ingot alloys demonstrated higher compressive strengths than the die-cast alloys across all conditions. At ε = 0.05, the ingot refined for 7 min with 80% scrap metal showed a strength of 424 MPa, compared with the die-cast alloy's 349 MPa under the same conditions. Similarly, at ε = 0.1, this ingot reached 523 MPa, while the die-cast alloy achieved 414 MPa. Among the ingot samples, the highest stress at ε = 0.1 was recorded for three variants: those refined for 7 and 9 min with 70% scrap, and the 7 min sample with 80% scrap—all reaching approximately 523 MPa. These results suggest that moderate scrap content combined with 7–9 min of refining yielded consistently high mechanical strength in ingot form. For die-cast samples, the best results at ε = 0.1 were observed in the sample refined for 15 min with 70% scrap (467 MPa), followed by the 9 min, 70% scrap sample (462 MPa). Although these values were slightly lower than their ingot counterparts, they still demonstrated high stress levels at advanced strain. Comparing the ingot and die-cast forms, the ingots consistently showed higher compressive strength and often lower standard deviations, indicating better uniformity. At 7 min and 70% scrap, the ingot's strength was 411 MPa (ε = 0.05) and 508 MPa (ε = 0.1), while the die-cast counterpart achieved 343 MPa and 460 MPa. The significant difference at ε = 0.05 highlights the superior consistency and strength retention of ingot materials over die-cast alloys, which may suffer from casting defects or porosity. Overall, lower scrap content, longer refining times, and ingot processing favored better mechanical performance, with ingots exhibiting not only higher strength but also greater consistency across various processing conditions. When comparing processing routes, numerous studies have demonstrated that ingot casting provides better mechanical properties than die casting due to improved control over solidification and reduced porosity [36]. Furthermore, in the literature, well-cast and treated aluminum–silicon alloys (e.g., AlSi9Cu3) typically exhibit yield strengths of 250–350 MPa and ultimate tensile strengths of 350–500 MPa in the die-cast state. When produced as ingots or through wrought processes, these alloys may exceed 500–600 MPa under optimized conditions, consistent with the current dataset [37].

The data underscore the role of refining time in stabilizing mechanical properties. Extending the refining time from 7 to 9 min generally enhanced the mechanical properties in both alloy forms. With 80% scrap metal, increasing the refining time from 7 to 9 min boosted the die-cast alloy's strength from 349 MPa to 380 MPa at ε = 0.05, and from 414 to 423 MPa at ε = 0.1. This trend was also evident in the ingot samples. However, an exception was observed for the ingot with 80% scrap content, where an increase in refining time resulted in a decrease in strength. Prolonged refining time is known to improve melt purity by reducing gas and non-metallic inclusions, as reported in multiple studies [38]. This leads to improved mechanical properties such as yield strength and ultimate tensile strength. On the other hand, high scrap content is known to increase impurity levels, particularly Fe, Si, and other residuals, promoting the formation of brittle intermetallic phases (such as Al-Fe-Si) that degrade ductility and tensile properties [35]. This was evident in both the ingot and die-cast alloys, according to the dataset; for instance, the ingot with 15 min refining and 80% scrap only reached around 465 MPa in stress (ε = 0.1) despite the extended refining, indicating that excessive scrap content imposes a limit to property enhancement. This observation is supported by the findings of Šmalc et al. [39], who investigated AlSi9Cu3

alloy with scrap return contents ranging from 0% to 100%. However, their samples were subjected to natural aging for 35 days prior to testing. They reported a gradual decline in mechanical strength beyond 60% scrap content, which was attributed to the formation of Fe-rich intermetallic phases that negatively affected the mechanical properties.

In the present study, although the influence of Mg content on mechanical properties was considered minor due to its overall low level and the consistent processing parameters, the literature data clearly demonstrate the significant role of Mg in Al–Si–Cu alloys. For example, in a study on Sr-modified Al–Si eutectic alloys with Mg contents ranging from 0.1 to 0.4 wt%, it was shown that Mg additions enhanced yield strength and ultimate tensile strength by up to 94% and 52%, respectively, while reducing elongation by approximately 40%, with the strengthening effect being most pronounced at lower Cu levels [40]. These effects were attributed to both solid solution and precipitation strengthening mechanisms. Similarly, in hypoeutectic Al–7%Si alloys, Mg additions in the range of 0.5–2.5 wt% led to significant refinement of primary α-Al dendrites and modification of the eutectic Si morphology, resulting in improved strength. However, at higher Mg contents, the formation of coarse Mg_2Si intermetallics reduced ductility [41]. Furthermore, detailed investigations on the heat treatment behavior of Al–Si–Cu–Mg alloys highlight the role of Mg in forming hardening phases such as Mg_2Si and Q-$Al_5Mg_8Si_6Cu_2$ and in influencing their dissolution and precipitation kinetics during T6 treatment, thereby impacting the final mechanical performance [42]. In contrast, the mechanical differences observed in the present work are more plausibly linked to variations in refining time and recycled content, rather than to minor fluctuations in Mg content.

The obtained results indicate that an appropriate refining time preserves high mechanical properties, even with a high scrap content. This may be attributed to the good distribution of phases in the microstructure and favorable microstructural conditions, such as fewer defects and evenly distributed silicon particles in the aluminum matrix. Samples with lower and higher recycled scrap content exhibited good mechanical properties, with a higher scrap content not necessarily compromising strength. The refining time emerged as a key factor in optimizing the alloy's microstructure, leading to high ultimate stress values and adequate plasticity, regardless of the scrap content [43].

Additionally, the obtained findings underscore the potential for significantly increasing recycled scrap content in aluminum production while maintaining mechanical integrity, reducing reliance on primary aluminum extraction and lowering overall energy consumption. However, achieving widespread adoption of such sustainable practices requires overcoming certain barriers, including concerns about alloy brittleness due to higher iron content and the need for process modifications to control porosity. If industries integrate optimized degassing and solidification control methods, they can enhance the quality and reliability of high-recycled-content aluminum alloys. Future research should focus on refining process parameters to mitigate iron-related issues and investigating alternative alloying strategies to further improve sustainability without sacrificing performance.

This study contributes to the goals of sustainable manufacturing by demonstrating the viability of using up to 80% recycled aluminum scrap without compromising material performance. By optimizing refining time and promoting the efficient use of secondary raw materials, the findings directly support the United Nations Sustainable Development Goal 12: Responsible Consumption and Production.

4. Conclusions

Based on the conducted research on barbotage of castings and ingots made of EN AC-46000 (AlSi9Cu3) alloy with varying amounts of recycled scrap, the following conclusions were formulated:

- Extending the barbotage process duration reduced the gas content in castings, leading to improved quality;
- The parameters of the barbotage process did not significantly affect the hardness of the investigated ingots and castings, ranging from 77 to 81 HB for ingots and 98 to 101 HB for castings;
- Refining time plays a critical role in determining mechanical performance. An optimal duration—typically between 7 and 9 min—can significantly enhance strength by improving melt quality;
- Increasing the proportion of recycled scrap metal generally results in reduced mechanical strength, particularly in die-cast alloys;
- When comparing ingot and die-cast alloys, ingot variants consistently demonstrate higher compressive strength and better uniformity, as indicated by lower standard deviations. This suggests greater structural integrity and fewer casting defects;
- Prolonged barbotage enhances microstructural homogenization, leading to improved mechanical properties of both castings and ingots. Additionally, a higher recycled scrap content, despite the increased presence of iron-rich phases, contributes to mechanical performance;
- The results demonstrate that a 9 min barbotage time offers an optimal balance between melt quality and economic efficiency, reducing inert gas consumption and equipment wear while maintaining mechanical performance even with high scrap content, making it particularly suitable for industrial implementation.

Author Contributions: Conceptualization, B.L.-M. and P.K.; methodology, B.L.-M.; formal analysis, B.L.-M. and A.W.; investigation, A.W., B.L.-M. and P.K.; writing—original draft preparation, B.L.-M. and P.K.; writing—review and editing, B.L.-M. and A.W.; visualization, B.L.-M. and P.K.; supervision, B.L.-M. and A.W. All authors have read and agreed to the published version of the manuscript.

Funding: This research received no external funding.

Institutional Review Board Statement: Not applicable.

Informed Consent Statement: Not applicable.

Data Availability Statement: The data presented in this study are available on request from the corresponding author.

Conflicts of Interest: The authors declare no conflicts of interest.

References

1. Wu, J.; Djavanroodi, F.; Gode, C.; Attarilar, S.; Ebrahimi, M. Melt Refining and Purification Processes in Al Alloys: A Comprehensive Study. *Mater. Res. Express* **2022**, *9*, 032001. [CrossRef]
2. Reddy, B.M.; Nallusamy, T. Degassing of Aluminum Metals and Its Alloys in Non-ferrous Foundry. In *Advances in Materials Research. ICAMR 2019*; Kumaresan, G., Shanmugam, N.S., Dhinakaran, V., Eds.; Springer Proceedings in Materials; Springer: Singapore, 2021; Volume 5, pp. 637–644. [CrossRef]
3. Gaustada, G.; Olivetti, E.; Kirchain, R. Improving Aluminum Recycling: A Survey of Sorting and Impurity Removal Technologies. *Resour. Conserv. Recycl.* **2012**, *58*, 79–87. [CrossRef]
4. Liu, Z.K. *Effect of Impurities on Alloys*; I. T. Program; Energy Efficiency and Renewable Energy, US Department of Energy: Washington, DC, USA, 2003.
5. Xetal, L. Study on Hydrogen Removal of AZ91 Alloys Using Ultrasonic Argon Degassing Process. *Ultrason. Sonochem.* **2015**, *26*, 73–80.
6. Zhang, Z.H.; Bian, X.F.; Liu, X.F. Heredity of Hydrogen in Al Alloys During Melting Process. *Mater. Sci. Forum* **2014**, *331–337*, 307–312. [CrossRef]
7. Tsuru, T.; Shimizu, K.; Yamaguchi, M.; Itakura, M.; Ebihara, K.; Bendo, A.; Toda, H. Hydrogen-Accelerated Spontaneous Microcracking in High-Strength Aluminium Alloys. *Sci. Rep.* **2020**, *10*, 1998. [CrossRef] [PubMed]

8. Zhou, M.; Shu, D.; Li, K.; Zhang, W.Y.; Sun, B.D.; Wang, J.; Ni, H.J. Performance Improvement of Industrial Pure Aluminum Treated by Stirring Molten Fluxes. *Mater. Sci. Eng. A* **2003**, *347*, 280–290. [CrossRef]
9. Bogdanova, T.A.; Merkulova, G.A.; Gilmanshina, T.R.; Kosovich, A.A.; Lytkina, S.I.; Cheglakov, A.V.; Antonov, M.M. Comparative Evaluation of Methods for Determination of Hydrogen and Non-Metallic Inclusions Content in Aluminum Alloys. *ARPN J. Eng. Appl. Sci.* **2021**, *16*, 355–360.
10. Mancilla, E. Comparison of the Hydrodynamic Performance of Rotor-Injector Devices in a Water Physical Model of an Aluminum Degassing Ladle. *Chem. Eng. Res. Des.* **2017**, *118*, 158–169. [CrossRef]
11. Kucharikova, L.; Tillova, E.; Bokuvka, O. Recycling and Properties of Recycled Aluminium Alloys Used in the Transportation Industry. *Transp. Probl.* **2016**, *11*, 117–122. [CrossRef]
12. Brough, D.; Jouhara, H. The Aluminium Industry: A Review on State-of-the-Art Technologies, Environmental Impacts, and Possibilities for Waste Heat Recovery. *Int. J. Thermofluids* **2020**, *1–2*, 100007. [CrossRef]
13. Yang, J.; Liu, B.; Shu, D.; Yang, Q.; Hu, T. Vehicle Giga-Casting Al Alloys Technologies, Applications, and Beyond. *J. Alloys Compd.* **2025**, *1013*, 178552. [CrossRef]
14. Chateau, J.M. Latest Trends in Molten Metal In-Line Treatment. *Alum. Times* **2003**, *04/05*, 34–35.
15. Gao, G.; Wang, M.; Shi, D.; Kang, Y. Simulation of Bubble Behavior in a Water Physical Model of an Aluminum Degassing Ladle Unit Employing Compound Technique of Rotary Blowing and Ultrasonic. *Metall. Mater. Trans. A* **2019**, *50*, 1997–2005. [CrossRef]
16. Warke, V.S.; Shankar, S.; Makhlouf, M.M. Mathematical Modeling and Computer Simulation of Molten Aluminum Cleaning by the Rotating Impeller Degasser: Part II. Removal of Hydrogen Gas and Solid Particles. *J. Mater. Process. Technol.* **2005**, *168*, 119–126. [CrossRef]
17. Wu, R.; Shu, D.; Sun, B.; Wang, J.; Li, F.; Chen, H.; Lu, Y. Theoretical Analysis and Experimental Study of Spray Degassing Method. *Mater. Sci. Eng. A* **2005**, *408*, 19–25. [CrossRef]
18. Mostafaei, M.; Ghobadi, M.; Eisaabadi, G.; Uludag, B.M.; Tiryakioglu, M. Evaluation of the Effects of Rotary Degassing Process Variables on the Quality of A357 Aluminum Alloy Castings. *Metall. Mater. Trans. B* **2016**, *47*, 3469–3475. [CrossRef]
19. Bhaskar, M.; Nalluswamy, T.S.; Suresh, P. Melt Treatment in Die Casting Industries. 29 April 2021, PREPRINT (Version 1). *Res. Sq.* **2021**. [CrossRef]
20. Gyarmati, G.; Fegyverneki, G.; Tokár, M.; Mende, T. The Effects of Rotary Degassing Treatments on the Melt Quality of an Al-Si Casting Alloy. *Int. J. Met.* **2020**, *15*, 141–151. [CrossRef]
21. Shabestari, S.G.; Mokarian, P.; Saeidinia, S. Effect of Process Variables in Rotary Degassing of Aluminum. *CIM Bull.* **2004**, *97*, 74.
22. Choongdo, L.; Taeil, S.; Kwangseon, S. Effect of Gas Bubbling Filtration Treatment on Microporosity Variation in A356 Aluminium Alloy. *Acta Metall. Sin. (Engl. Lett.)* **2016**, *29*, 638–646. [CrossRef]
23. *PN-EN 1706+A1:2022-01*; Aluminium and Aluminium Alloys—Castings—Chemical Composition and Mechanical Properties. PKN Polish Committee for Standardization: Warsaw, Poland, 2022.
24. *ASTM E10-18*; Standard Test Method for Brinell Hardne27of Metallic Materials. ASTM International: West Conshohocken, PA, USA, 2017.
25. *ASTM E9-09*; Standard Test Methods of Compression Testing of Metallic Materials at Room Temperature. ASTM International: West Conshohocken, PA, USA, 2009.
26. Kulikov, B.; Partyko, E.; Kosovich, A.; Yuryev, P.; Mansurov, Y.; Stepanenko, N.; Baykovskiy, Y.; Bozhko, D.; Durnopyanov, A.; Dombrovskiy, N.; et al. Analysis of Composition, Properties, and Usage Efficiency of Different Commercial Salt Fluxes for Aluminum Alloy Refining. *Metals* **2025**, *15*, 448. [CrossRef]
27. Gumienny, G.; Pisarek, B.; Szymczak, T.; Gawroński, J.; Just, P.; Władysiak, R.; Rapiejko, C.; Pacyniak, T. Effect of Degassing Parameters on Mechanical Properties of EN AC-46000 Gravity Die Castings. *Materials* **2022**, *15*, 8323. [CrossRef]
28. Lazaro-Nebreda, J.; Patel, J.B.; Lordan, E.; Zhang, Y.; Karakulak, E.; Al-Helal, K.; Scamans, G.M.; Fan, Z. Degassing of Aluminum Alloy Melts by High Shear Melt Conditioning Technology: An Overview. *Metals* **2022**, *12*, 1772. [CrossRef]
29. Socha, L.; Prášil, T.; Gryc, K.; Svizelova, J.; Saternus, M.; Merder, T.; Nuska, P. Assessment of Refining Efficiency during the Refining Cycle in a Foundry Degassing Unit in Industrial Conditions. *Sci. Rep.* **2024**, *14*, 1415. [CrossRef]
30. Liu, H.; Bouchard, M.; Zhang, L. An Experimental Study of Hydrogen Solubility in Liquid Aluminium. *J. Mater. Sci.* **1995**, *30*, 4309–4315. [CrossRef]
31. Prášil, T.; Socha, L.; Gryc, K.; Svizelová, J.; Saternus, M.; Merder, T.; Gráf, M. Using Physical Modeling to Optimize the Aluminium Refining Process. *Materials* **2022**, *15*, 7385. [CrossRef]
32. Wang, Q.G.; Crepeau, P.N.; Davidson, C.J.; Griffiths, J.R. Oxide Films, Pores, and the Fatigue Lives of Cast Aluminum Alloys. *Metall. Mater. Trans. B* **2006**, *37*, 887–895. [CrossRef]
33. Jang, H.S.; Kang, H.J.; Yoon, P.; Lee, G.; Jeon, J.B.; Park, J.Y.; Kim, E.S.; Shin, S. Effects of Mg Content on Hydrogen Content and Melt Quality of Al-Mg Alloys. *Metals* **2019**, *9*, 1235. [CrossRef]
34. Ganesh, M.S.; Reghunath, N.; JLevin, M.; Prasad, A.; Doondi, S.; Shankar, K.V. Strontium in Al–Si–Mg Alloy: A Review. *Met. Mater. Int.* **2022**, *28*, 1–40. [CrossRef]

35. Piatkowski, J.; Nowinska, K.; Matula, T.; Siwiec, G.; Szucki, M.; Oleksiak, B. Microstructure and Mechanical Properties of AlSi10MnMg Alloy with Increased Content of Recycled Scrap. *Materials* **2025**, *18*, 1119. [CrossRef]
36. Raabe, D.; Ponge, D.; Uggowitzer, P.J.; Roscher, M.; Paolantonio, M.; Liu, C.; Antrekowitsch, H.; Kozeschnik, E.; Seidmann, D.; Gault, B.; et al. Making Sustainable Aluminum by Recycling Scrap: The Science of "Dirty" Alloys. *Prog. Mater. Sci.* **2022**, *128*, 100947. [CrossRef]
37. Mrówka-Nowotnik, G.; Gancarczyk, K.; Nowotnik, A.; Dychtoń, K.; Boczkal, G. Microstructure and Properties of As-Cast and Heat-Treated 2017A Aluminium Alloy Obtained from Scrap Recycling. *Materials* **2021**, *14*, 89. [CrossRef]
38. Podaril, M.; Prášil, T.; Majernik, J.; Kampf, R.; Socha, L.; Gryc, K.; Gráf, M. Aluminum Melt Degassing Process Evaluation Depending on the Design and the Degree of the FDU Unit Graphite Rotor Wear. *Materials* **2022**, *15*, 4924. [CrossRef]
39. Šmalc, J.; Vončina, M.; Mrvar, P.; Balaško, T.; Krutiš, V.; Petrič, M. The Influence of Foundry Scrap Returns on Chemical Composition and Microstructure Development of $AlSi_9Cu_3$ Alloy. *Crystals* **2023**, *13*, 757. [CrossRef]
40. Moustafa, M.A.; Samuel, F.H.; Doty, H.W.; Valtierra, S. Effect of Mg and Cu additions on the microstructural characteristics and tensile properties of Sr-modified Al–Si eutectic alloys. *Int. J. Cast Met. Res.* **2002**, *14*, 235–253. [CrossRef]
41. Li, Q.; Li, B.; Li, J.; Xia, T.; Lan, Y.; Guo, T. Effects of the Addition of Mg on the Microstructure and Mechanical Properties of Hypoeutectic Al–7%Si Alloy. *Int. J. Met.* **2017**, *11*, 823–832. [CrossRef]
42. Sjölander, E.; Seifeddine, S. The heat treatment of Al–Si–Cu–Mg casting alloys. *J. Mater. Process. Technol.* **2010**, *210*, 1249–1259. [CrossRef]
43. Bell, S.; Davis, B.; Javaid, A.; Essadiqi, E. Final Report on Refining Technologies of Aluminum. *Report No. 2003-21(CF)*. 2023. Available online: https://ressources-naturelles.canada.ca/sites/www.nrcan.gc.ca/files/mineralsmetals/pdf/mms-smm/busi-indu/rad-rad/pdf/2003-21(cf)cc-eng.pdf (accessed on 19 May 2025).

Disclaimer/Publisher's Note: The statements, opinions and data contained in all publications are solely those of the individual author(s) and contributor(s) and not of MDPI and/or the editor(s). MDPI and/or the editor(s) disclaim responsibility for any injury to people or property resulting from any ideas, methods, instructions or products referred to in the content.